TITLE

Cell type-specific effects of isoflurane on two distinct afferent inputs to cortical layer 1.

AUTHORS AND AFFILIATIONS

Caitlin A. Murphy[1]
Matthew I. Banks[1]
[1]Department of Anesthesiology, University of Wisconsin, Madison, Wisconsin

Corresponding Author:
Caitlin A. Murphy
caitlin.murphy@wisc.edu
Tel: (608) 263-5552

KEYWORDS

anesthesia; isoflurane; electrophysiology; neocortex; thalamus; optogenetics; interneurons; pyramidal cells; patch-clamp techniques

ABSTRACT

While their behavioral effects are well-characterized, the mechanisms by which anesthetics induce loss of consciousness are largely unknown. Anesthetics may disrupt integration and propagation of information in corticothalamic networks. Recent studies have shown that isoflurane diminishes synaptic responses of thalamocortical (TC) and corticocortical (CC) afferents in a pathway-specific manner. However, whether the synaptic effects of isoflurane observed in extracellular recordings persist at the cellular level has yet to be explored. Here, we activate TC and CC layer 1 inputs in non-primary mouse neocortex in ex vivo brain slices and explore the degree to which isoflurane modulates synaptic responses in pyramidal cells and in two inhibitory cell populations, somatostatin-positive (SOM+) and parvalbumin-positive (PV+) interneurons. We show that the effects of isoflurane on synaptic responses and intrinsic properties of these cells varies among cell type and by cortical layer. Layer 1 inputs to L4 pyramidal cells were suppressed by isoflurane at both TC and CC synapses, while those to L2/3 pyramidal cells and PV+ interneurons were not. TC inputs to SOM+ cells were rarely observed at all, while CC inputs to SOM+ interneurons were robustly suppressed by isoflurane. These results suggest a mechanism by which isoflurane disrupts integration and propagation of incoming cortical signals.

INTRODUCTION

Anesthetics may ultimately influence both the level and contents of consciousness via actions on corticothalamic circuits, disrupting integration of information throughout the cortical hierarchy (Crick and Koch, 2003; Dehaene and Changeux, 2011; Koch et al., 2016). Activity in higher order cortical areas is particularly sensitive to anesthetics (Nourski et al., 2017; Nourski et al., 2018), as is corticocortical (CC) feedback connectivity (Ferrarelli et al., 2010; Boly et al., 2012; Liu et al., 2012; Raz et al., 2014; Mashour and Hudetz, 2017; Murphy et al., 2019). In addition to cortical effects, higher order thalamocortical (TC) connectivity is suppressed during both sleep (Picchioni et al., 2014) and anesthesia (Langsjo et al., 2012; Liu et al., 2013; Akeju et al., 2014). Activation of non-specific thalamic nuclei during anesthetic-induced unconsciousness (Redinbaugh et al., 2020) and non-REM sleep (Honjoh et al., 2018) promotes behavioral arousal, implicating higher order thalamic centers as enablers of consciousness.

Recent studies from our lab have shown that in *ex vivo* slices, isoflurane diminishes synaptic responses in a pathway-specific manner (Raz et al., 2014; Murphy et al., 2019). Despite overlapping terminal fields in layer 1, CC feedback afferents to a non-primary cortical area were preferentially suppressed by isoflurane compared to non-primary TC inputs. However, extracellular recordings used in these investigations capture summed effects across all synapses, leaving open questions as to whether observed effects are consistent across post-synaptic targets. For example, differential effects on inhibitory interneurons compared to excitatory cells may shift the balance of excitation and inhibition (Haider et al., 2013; Xue et al., 2014), disrupting integration of inputs in pyramidal cell dendrites or constraining the output of the cortical column. Superficial and deep layers may operate within functionally separate domains, where cells in superficial layers primarily carry out intracortical interactions, and those in deep layers facilitate interactions with lower cortical and subcortical targets in the

60 feedback direction (Douglas et al., 1989; Douglas and Martin, 2004; Douglas and Martin, 2007;
61 Binzegger et al., 2009). Differential effects of anesthetics on cells residing in different layers
62 may provide insight into the functional roles of discrete cortical networks and the mechanisms
63 that subserve the breakdown of connectivity observed during anesthesia.

64 Here, we investigate the effect of isoflurane on independently activated TC and CC
65 inputs to layer 1 of non-primary neocortex in brain slices. We evaluate the pathway- and cell
66 type-specific effects of isoflurane on synaptic responses recorded in pyramidal cells in layers
67 2-5 and in two subpopulations of inhibitory cells, SOM+ and PV+ interneurons.

68

69 **METHODS**

70 To express the fluorescent reporter tdTomato in non-overlapping populations of GABAergic
71 interneurons, homozyogous, Cre-dependent tdTomato male mice were bred with either SOM-
72 Cre female or PV-Cre female mice; heterozygous offspring (both sexes) were used for all
73 experiments. Viral constructs containing channelrhodopsin-2 (ChR2) and fluorescent reporter
74 YFP (AAV2-hSyn-hChR2(H134R)-eYFP; provided by K. Deisseroth, Stanford University via
75 University of North Carolina Vector Core) were injected into either posterior medial thalamus
76 (AP: -2.25 mm, ML: 1.25 mm, DV: -3.35 mm; volume: 1 μL) or cingulate cortex (AP: 0.2 mm,
77 ML: 0.3 mm, DV: 0.9 mm; volume: 1 μL) to independently activate non-primary TC and CC
78 feedback afferents, respectively.

79 After allowing at least 3 weeks for expression of the virus, acute coronal brain slices
80 containing were collected and recordings were made from medial secondary visual cortex.
81 Intracellular whole cell patch clamp recordings were conducted in current clamp mode from
82 pyramidal cells in layers 2-5, SOM+ interneurons, or PV+ interneurons; extracellular
83 multichannel recordings were collected concurrently. Cell types were identified either by Cre-

84 dependent expression of td-Tomato reporter (for SOM+ and PV+ interneurons) or by
85 morphology (pyramidal cells). To further guide identification of cell types, each cell's response
86 to 600 msec current steps was evaluated as previously described (Krause et al., 2017). All
87 signals were low-pass filtered at 10 kHz and digitized at 40 kHz.

88 To activate either TC or CC afferents, blue light was delivered exclusively to layer 1 (150
89 µm diameter, 470 nm; Polygon400, Mightex Systems, Toronto, Ontario). For each trial,
90 synaptic responses were evoked using four brief pulses of light (2 msec; 10 Hz) at one of at
91 least five light intensities randomly selected from a range of intensities (0.022-2.2 mW). Each
92 trial was separated by ten seconds, and at least eight trials were conducted for each light
93 intensity, randomly interleaved.

94 Signals from each of 16 extracellular channels were filtered (bandpass filter, 1-300Hz) to
95 yield local field potentials used to calculate the current source density (CSD; (Mitzdorf, 1985))
96 with the spline inverse method (Pettersen et al., 2006). The signal in layer 1 with the shortest
97 latency current sink (inward transmembrane current) was used for further analysis. Intracellular
98 signals were filtered (bandpass filter, 0.1-1000 Hz), and responses were averaged across trials
99 of the same stimulus intensity. Responses to a single stimulus intensity were selected for
100 detailed analysis; the intensity selected was the minimum light intensity for which at least 50%
101 of trials (8-10 trials per intensity) evoked a response with <1 msec latency jitter.

102 Response amplitude was defined as the peak of the signal within 50 msec of the stimulus
103 (first pulse only). Paired pulse ratio was computed for intracellular recordings, calculated by
104 dividing the post-synaptic potential (PSP) amplitude of the second pulse by the PSP amplitude
105 of first pulse. TC- and CC-evoked responses were compared across control, isoflurane (0.24-
106 0.29 mM), and recovery conditions. To exclude the possibility that effects of isoflurane were
107 due to response degradation over time, the average of control and recovery measures were
108 used as a baseline for comparison to isoflurane.

109 A linear mixed effects model was used to evaluate the pathway- and cell type-dependent
110 effects of isoflurane on intrinsic and evoked response properties of individual cells. Fixed
111 effects were cell type (L2/3 Pyr, L4 Pyr, L5 Pyr, SOM+, or PV+) and drug condition (baseline or
112 isoflurane), as well as afferent pathway (TC or CC) for evoked responses. Interaction terms
113 between isoflurane and each of the other fixed effects were also included, as well as a three-
114 way interaction term representing interactions between cell type and pathway of drug effects;
115 random effects were slice experiment and cell with random slopes for drug condition. For PSP
116 amplitude and input resistance measures, heteroscedasticity was corrected by log
117 transforming response variables, and effects are reported as percent changes. To allow for
118 direct comparison among cell types and pathways, all isoflurane effects are reported relative to
119 baseline.
120

121 **RESULTS**

122 *Activation of TC and CC inputs to layer 1 elicit short-latency synaptic responses*

123 Synaptic responses from TC and CC afferents were elicited by activating channelrhodopsin in
124 afferent axon terminals in layer 1. Brief pulses of light evoked short latency current sinks in
125 layer 1 (Table 1). No effect of afferent pathway was observed for baseline amplitude ($t(29) =$
126 0.41, $p=0.69$) or latency ($t(29) = 0.26$, $P = 0.80$) of layer 1 current sinks. Evoked currents in
127 layer 1 precipitated PSPs in pyramidal cells in layers 2-5 (Table 2; Figure 2B,D), and in SOM+
128 and PV+ cells (Table 2; Figure 4B,D,F).

129 Main effects of pathway and cell type on amplitudes of synaptic responses were tested.
130 A 2-way ANOVA was not significant for effects of pathway ($F(1,47) = 0.07$, $P=0.79$) nor target
131 cell population ($F(4,47) = 1.68$, $P=0.17$), suggesting no differences in baseline (i.e., in the
132 absence of isoflurane) amplitudes among recorded cells. Similarly, no significant effect on

133 latency was observed for main effects of pathway ($F(1,47) = 1.00$, $P=0.32$) nor cell type
134 ($F(4,47) =1.68$, $P=0.17$).
135
136 *Isoflurane suppresses layer 1 current sinks elicited by CC inputs, but not TC inputs*
137 Despite their overlapping terminal fields and similar synaptic dynamics under control
138 conditions, TC and CC inputs to layer 1 were differentially affected by isoflurane (Figure 1;
139 Table 1), consistent with previous results from our lab (Murphy et al., 2019). Amplitudes of
140 layer 1 current sinks were suppressed by isoflurane by 21.8% for CC inputs, while current
141 sinks evoked by TC inputs were relatively resistant to isoflurane (Figure 1; Table 1).
142
143 *Isoflurane suppresses synaptic responses in a cell type-dependent manner*
144 Current sinks isolated from current source densities represent averages of inward-going
145 transmembrane currents across all synapses. However, evidence suggests that the synaptic
146 properties – and therefore potential functional roles – of TC versus CC inputs to may be cell
147 type- and layer-dependent (Cruikshank et al., 2012; Sermet et al., 2019). Therefore, we sought
148 to investigate whether the effects of isoflurane on layer 1 current sinks were uniform for all
149 post-synaptic targets of each afferent pathway, or whether certain cell populations were
150 differentially sensitive to isoflurane.
151 We evaluated the degree to which isoflurane modulated the amplitudes of post-synaptic
152 potentials elicited by layer 1 afferents in $L^2/_3$, L4, and L5 pyramidal cells (Figure 2) as well as
153 SOM+ and PV+ cells (Figure 4). Independent of any interactions of cell type or afferent
154 pathway, isoflurane significantly suppressed evoked post-synaptic potentials of target cells
155 ($\chi(1) = 16.6$, $P<0.0001$). Contrary to our findings for extracellularly recorded layer 1 current
156 sinks, we found no significant interaction of pathway on the effect of isoflurane ($\chi(1) = 2.00$,
157 $P=0.16$). However, the effect of isoflurane was significantly dependent on cell type ($\chi(4) =$

158 17.862, P=0.0013). The interaction between cell type and pathway was not significant ($\chi(1)$ =
159 6.52, P=0.16). In other words, the effect of isoflurane is cell type-dependent, and within each
160 cell type, no significant differences were observed between afferent pathways.

161 Amplitudes of synaptic responses in L2/3 cells were not significantly affected by
162 isoflurane for either TC or CC inputs (Figure 2B,D; Figure 3; Table 3). Conversely, amplitudes
163 of synaptic responses in L4 cells were significantly suppressed by isoflurane for both TC and
164 CC inputs, to approximately the same degree (Figure 2B,D; Figure 3; Table 3). Isoflurane also
165 suppressed CC inputs, but not TC inputs, to L5 pyramidal cells (Figure 2D; Figure 3; Table 3),
166 though this effect was not significantly different between pathways (P=0.19).

167 In addition to providing input to pyramidal cells, long-range TC and CC projections also
168 target inhibitory interneurons. We were also interested in the effect of isoflurane on evoked
169 responses in two subpopulations of inhibitory cells, SOM+ and PV+ interneurons, and whether
170 these effects were different than those observed for pyramidal cell populations. Consistent with
171 previous studies (Beierlein et al., 2003; Cruikshank et al., 2010; Audette et al., 2018) and our
172 own observations, TC inputs rarely elicited synaptic responses in SOM+ cells (n=2 cells); as
173 such, isoflurane effects on TC inputs to SOM+ cells are not reported. Activation of CC
174 afferents, however, reliably elicited synaptic responses in SOM+ cells (Figure 4). These
175 synapses were particularly sensitive to isoflurane; amplitudes of synaptic responses for CC
176 inputs to SOM+ cells were suppressed 35.8% during isoflurane compared to baseline (Table
177 3). Conversely, no effect of isoflurane on amplitudes of responses in PV+ cells was detected
178 for either afferent pathway (Table 3). Thus, even among subpopulations of GABAergic
179 interneurons, the effect of isoflurane on CC responses was significantly different (-35.8% for
180 SOM+ cells versus -10.0% for PV+ cells, P=0.014; Figure 5), suggesting distinct roles of each
181 cell type during anesthesia.

182

183 *Pre- and post-synaptic effects of isoflurane are cell type-dependent*

184 A multitude of cellular and synaptic dynamics may underlie changes in neural activity observed
185 during anesthesia. For example, effects of isoflurane on synaptic responses as we describe
186 here may manifest as a result of pre-synaptic effects of isoflurane (e.g., effects on calcium
187 influx or vesicle release) (Baumgart et al., 2015), on discrete intrinsic properties of post-
188 synaptic cells that give rise to changes in their excitability, or a combination of pre- and post-
189 synaptic effects. Although we cannot ascribe the contributions of specific synaptic or intrinsic
190 effects of isoflurane to observed effects on evoked responses, characterizing isoflurane-
191 induced changes in synaptic plasticity or intrinsic properties of post-synaptic cells may provide
192 insight into the complicated interactions of network components during anesthesia. To this
193 end, we evaluated the extent to which isoflurane modulated paired pulse ratios and intrinsic
194 membrane properties (resting membrane potential, input resistance, membrane time constant,
195 and spike threshold) of each cell. Baseline values for paired pulse ratio and intrinsic membrane
196 properties are displayed in Table 2 and Table 4, respectively; effects of isoflurane are
197 described below and in figures and tables as changes relative to baseline.

198 Isoflurane significantly enhanced the paired pulse ratio of CC inputs to SOM+ cells but
199 had no effect on paired pulse ratios for other pathway-cell type combinations (Figure 6; Table
200 5). Intrinsic membrane properties of L4 pyramidal cells were especially sensitive to isoflurane.
201 In L4 pyramidal cells, input resistance was 13.5% lower and membrane time constants 27.8%
202 shorter during isoflurane relative to baseline; isoflurane did not affect input resistance nor time
203 constants of any other cell type (Figure 7). Isoflurane also reduced resting membrane potential
204 in L4 and L5 pyramidal cells (Figure 7). Effects of isoflurane observed in L4 pyramidal cells
205 were accompanied by a decrease in spike threshold (Figure 7).

206

207 **DISCUSSION**

208 In these experiments, we describe the effects of isoflurane on synaptic responses and intrinsic
209 membrane properties of pyramidal cells in layers 2-5, as well as in SOM+ and PV+
210 interneurons. Previous investigations of the effects of isoflurane on synaptic responses have
211 suggested that CC feedback inputs are suppressed to a greater extent than TC and CC
212 feedforward inputs (Raz et al., 2014; Murphy et al., 2019). Here, we show that suppression of
213 extracellular synaptic responses is pathway-dependent, recapitulating previous findings using
214 a similar experimental paradigm (Raz et al., 2014; Murphy et al., 2019). We also demonstrate
215 that the suppression of synaptic responses by isoflurane is cell type- and layer-dependent,
216 providing insight into the mesocircuit-level mechanisms underlying the mechanisms of
217 anesthesia.
218
219 *Resistance of PV+ interneurons to isoflurane suggests shift in E/I balance*
220 We show that synaptic responses of PV+ interneurons to both TC and CC inputs are resistant
221 to suppression during isoflurane. TC input to PV+ cells provides stimulus-locked fast
222 feedforward-inhibition to pyramidal cells, restricting the window of opportunity for generating
223 spikes and improving spike timing among populations of pyramidal cells (Pouille and
224 Scanziani, 2001; Krause et al., 2017). We propose that the relative insensitivity of fast-spiking
225 PV+ neurons to isoflurane we observe here may underlie previous observations from our lab
226 and others. That is, early responses of the cortical network to TC inputs are relatively
227 preserved during isoflurane, while recurrent, propagating network activity is highly sensitive
228 (Hentschke et al., 2017; Murphy et al., 2017). Although we report activity of single cells only in
229 our study, the relative preservation of PV+ cell responses during isoflurane is likely to shift the
230 E/I balance in the network toward inhibition. PV+ cells are known to be important for mediating
231 E/I balance within cortical networks (Dichter and Ayala, 1987; Ferguson and Gao, 2018).
232 Pyramidal cells in L2/3, for example, receive PV+ cell-mediated inhibitory input proportional to

233 their excitation under normal conditions, and changes in input to pyramidal cells – as we
234 observe in L4 cells in our experiments – without commensurate changes in PV+ cells disrupts
235 this E/I balance (Xue et al., 2014). If these cell type-specific effects of isoflurane occur in
236 multiple cortical areas, shifts in local E/I balance may compound, contributing to the
237 progressive failure of information to be passed from one cortical area to the next.
238

239 *Suppression of L4 pyramidal cells during isoflurane may disrupt feedforward processing*
240 We show that synaptic responses of L4 pyramidal cells are suppressed during isoflurane for
241 responses evoked by both TC and CC inputs. That TC inputs to any cell type would be
242 affected by isoflurane is somewhat surprising, and that this effect would be exclusively
243 observed in L4 pyramidal cells is even more unexpected. L4 pyramidal cells are typically
244 considered mediators for propagating feedforward information, receiving sensory-specific
245 information from thalamus and lower areas (Cruikshank et al., 2010; Covic and Sherman,
246 2011; De Pasquale and Sherman, 2011; Viaene et al., 2011a; Viaene et al., 2011b) and
247 targeting L2/3 for output to higher areas (Xu et al., 2016; Meyer et al., 2018). Feedforward
248 circuits are relatively resistant to anesthetics (Lee et al., 2013; Raz et al., 2014; Murphy et al.,
249 2019) (though, see (Maksimow et al., 2014; Sanders et al., 2018)), and we show here that
250 extracellular recordings of current sinks evoked by activation of TC afferents were not affected
251 by isoflurane (Figure 1). Yet, interestingly, our results show that inputs to L4 cells are
252 preferentially suppressed by isoflurane, suggesting that suppression of TC and CC inputs
253 together may disrupt feedforward signaling.
254 While pre-synaptic mechanisms of isoflurane have been well-described (Herring et al.,
255 2009; Xie et al., 2013; Baumgart et al., 2015), our observations suggest that the mechanisms
256 underlying isoflurane effects in L4 pyramidal cells were not limited to pre-synaptic effects. No

257 changes in short-term synaptic plasticity were observed at these synapses (Figure 6), and TC
258 and CC inputs to L4 pyramidal cells were suppressed to a similar extent (Figure 3). However,
259 L4 pyramidal cells were significantly leakier during isoflurane, as evidenced by lower input
260 resistances and shorter membrane time constants relative to baseline (Figure 7). Not only
261 might these effects dampen voltage changes evoked by synaptic currents, but they are likely to
262 also contribute to the overall excitability of L4 cells, thereby attenuating their contributions to
263 processing of cortical signals.

264

265 *Evidence for disruption of predictive coding schemes during anesthesia*

266 In the present study, we find that isoflurane suppresses CC feedback afferents to L4 and L5
267 pyramidal cells (Figure 3) as well as those to dendrite-targeting SOM+ interneurons (Figure 5),
268 consistent with previous studies showing sensitivity of feedback connections during anesthesia
269 (Boly et al., 2012; Liu et al., 2012; Raz et al., 2014; Mashour and Hudetz, 2017; Murphy et al.,
270 2019). Feedback activation of the cortical column is mediated largely by intracortical afferents
271 to layer 1 that target distal dendrites of pyramidal cells. Dendritic calcium currents activated by
272 these inputs increase the gain of the input/output relationship of cortical pyramidal cells and
273 are highly correlated with sensory perception (Manita et al., 2015; Takahashi et al., 2016). This
274 process is tightly regulated by powerful disynaptic inhibition from SOM+ interneurons
275 (Murayama et al., 2009). Our observation that inputs to both SOM+ cells and infragranular
276 pyramidal cells are preferentially suppressed notably intersects with these previous findings in
277 the context of sensory coding. Suppression of intracortical feedback inputs to two key players
278 in this integration process may therefore disrupt the typical input/output function of pyramidal
279 cells.

Disruption of integration of inputs to L5 pyramidal cells is also consistent with what might be expected under anesthesia in the context of current theoretical models. The predictive coding hypothesis, for example, has often been used as a framework for understanding consciousness and sensory processing (Friston, 2005; Bastos et al., 2012; Clark, 2013). Under the predictive coding hypothesis, feedback signals must activate inhibition to offset incoming excitatory signals and prevent propagation of the excitatory, ascending error signal. Discrepancies between internally generated predictions and sensory input from external sources are propagated as excitatory “error signals”. Our data provide further evidence that multiple components of the predictive coding architecture may be disrupted by anesthesia. First, integration of predictions carried by feedback afferents may be perturbed, as feedback inputs to both SOM+ cells and L5 pyramidal cells – key mediators of feedback modulation of sensory responses – are altered by isoflurane. Second, propagation of error signals in the feedforward direction may be disrupted, as both TC and CC inputs to L4 cells – which mediate intracortical feedforward signals – are suppressed by isoflurane. Our data may demonstrate physiological correlates of components of the predictive coding model and provide insight into the disruption of sensory processing during anesthesia.

Future Directions

In these experiments, we investigate the effect of isoflurane on discrete components of a higher order cortical circuit. Investigating the pathway-, cell type-, and layer-specific effects of isoflurane is imperative for understanding the larger systems in which these components operate. Our findings will inform future investigations of sensory processing and changes in consciousness during anesthesia. Although here we activated inputs to layer 1 independently, future experiments *in vivo* will provide insight into how overlapping inputs to layer 1 affect arousal and sensory processing. It is reasonable to expect that the combined effects of

305 isoflurane on TC and CC inputs, for example, may engender supralinear effects on underlying
306 circuit components, synergistically contributing to disruption of sensory processing. Moreover,
307 *in vivo* investigations, such as those that involve artificially manipulating activity in different cell
308 types during anesthesia, may allow for causal, detailed descriptions of the pathway- and cell
309 type-specific components that are necessary and/or sufficient for consciousness. Lastly, a
310 recent study by Suzuki and Larkum (2020) suggests that anesthetics may prevent integration
311 of feedback signals by targeting signal amplification in apical dendrites of pyramidal cells, and
312 implies that this process may be mediated by metabotropic glutamate and cholinergic
313 receptors(Suzuki and Larkum, 2020). Future investigations should probe the extent to which
314 distinct inputs to layer 1 engage metabotropic glutamate or cholinergic systems, and how the
315 synaptic effects of anesthetics on layer 1 contributes to disruption of input-output computations
316 by anesthetics.
317

318 **ACKNOWLEDGEMENTS**

319 This work was supported by the National Institutes of Health (R01 GM109086 to MIB) and the
320 Department of Anesthesiology, School of Medicine and Public Health, University of Wisconsin,
321 Madison, WI, USA. The authors would also like to thank Bryan Krause for insight provided for
322 the statistical analyses conducted in this study, and Sean Grady for technical support.
323

324 **DISCLOSURES**

325 The authors have nothing to disclose.
326

327 **REFERENCES**

328 Akeju O, Loggia ML, Catana C, Pavone KJ, Vazquez R, Rhee J, Contreras Ramirez V,
329 Chonde DB, Izquierdo-Garcia D, Arabasz G, Hsu S, Habeeb K, Hooker JM, Napadow

330 V, Brown EN, Purdon PL (2014) Disruption of thalamic functional connectivity is a
331 neural correlate of dexmedetomidine-induced unconsciousness. Elife 3:e04499.

332

333 Audette NJ, Urban-Ciecko J, Matsushita M, Barth AL (2018) POm Thalamocortical Input
334 Drives Layer-Specific Microcircuits in Somatosensory Cortex. Cereb Cortex 28:1312-
335 1328.

336

337 Bastos AM, Usrey WM, Adams RA, Mangun GR, Fries P, Friston KJ (2012) Canonical
338 microcircuits for predictive coding. Neuron 76:695-711.

339

340 Baumgart JP, Zhou ZY, Hara M, Cook DC, Hoppa MB, Ryan TA, Hemmings HC, Jr. (2015)
341 Isoflurane inhibits synaptic vesicle exocytosis through reduced Ca2+ influx, not Ca2+-
342 exocytosis coupling. Proc Natl Acad Sci U S A 112:11959-11964.

343

344 Beierlein M, Gibson JR, Connors BW (2003) Two dynamically distinct inhibitory networks in
345 layer 4 of the neocortex. Journal of Neurophysiology 90:2987-3000.

346

347 Binzegger T, Douglas RJ, Martin KA (2009) Topology and dynamics of the canonical circuit of
348 cat V1. Neural Netw 22:1071-1078.

349

350 Boly M, Moran R, Murphy M, Boveroux P, Bruno MA, Noirhomme Q, Ledoux D, Bonhomme V,
351 Brichant JF, Tononi G, Laureys S, Friston K (2012) Connectivity changes underlying
352 spectral EEG changes during propofol-induced loss of consciousness. J Neurosci
353 32:7082-7090.

354

355 Clark A (2013) Whatever next? Predictive brains, situated agents, and the future of cognitive
356 science. Behav Brain Sci 36:181-204.

357

358 Covic EN, Sherman SM (2011) Synaptic properties of connections between the primary and
359 secondary auditory cortices in mice. CerebCortex 21:2425-2441.

360

361 Crick F, Koch C (2003) A framework for consciousness. Nat Neurosci 6:119-126.

362

363 Cruikshank SJ, Urabe H, Nurmikko AV, Connors BW (2010) Pathway-Specific Feedforward
364 Circuits between Thalamus and Neocortex Revealed by Selective Optical Stimulation of
365 Axons. Neuron 65:230-245.

366

367 Cruikshank SJ, Ahmed OJ, Stevens TR, Patrick SL, Gonzalez AN, Elmaleh M, Connors BW
368 (2012) Thalamic Control of Layer 1 Circuits in Prefrontal Cortex. The Journal of
369 Neuroscience 32:17813-17823.

370

De Pasquale R, Sherman SM (2011) Synaptic properties of corticocortical connections between the primary and secondary visual cortical areas in the mouse. JNeurosci 31:16494-16506.

Dehaene S, Changeux JP (2011) Experimental and theoretical approaches to conscious processing. Neuron 70:200-227.

Dichter MA, Ayala GF (1987) Cellular mechanisms of epilepsy: a status report. Science 237:157-164.

Douglas RJ, Martin KA (2004) Neuronal circuits of the neocortex. AnnuRevNeurosci 27:419-451.

Douglas RJ, Martin KAC (2007) Recurrent neuronal circuits in the neocortex. Current Biology 17:R496-R500.

Douglas RJ, Martin KAC, Whitteridge D (1989) A canonical microcircuit for neocortex. Neural Computation 1:480-488.

Ferguson BR, Gao W-J (2018) PV Interneurons: Critical Regulators of E/I Balance for Prefrontal Cortex-Dependent Behavior and Psychiatric Disorders. Frontiers in Neural Circuits 12.

Ferrarelli F, Massimini M, Sarasso S, Casali A, Riedner BA, Angelini G, Tononi G, Pearce RA (2010) Breakdown in cortical effective connectivity during midazolam-induced loss of consciousness. Proc Natl Acad Sci USA 107:2681-2686.

Friston K (2005) A theory of cortical responses. Philos Trans R Soc Lond B Biol Sci 360:815-836.

Haider B, Häusser M, Carandini M (2013) Inhibition dominates sensory responses in the awake cortex. Nature 493:97-100.

Hentschke H, Raz A, Krause BM, Murphy CA, Banks MI (2017) Disruption of cortical network activity by the general anesthetic isoflurane. Br J Anaesth 119:685-696.

Herring BE, Xie Z, Marks J, Fox AP (2009) Isoflurane inhibits the neurotransmitter release machinery. J Neurophysiol 102:1265-1273.

Honjoh S, Sasai S, Schiereck SS, Nagai H, Tononi G, Cirelli C (2018) Regulation of cortical activity and arousal by the matrix cells of the ventromedial thalamic nucleus. Nature Communications 9:2100.

Koch C, Massimini M, Boly M, Tononi G (2016) Neural correlates of consciousness: progress and problems. Nat Rev Neurosci 17:307-321.

Krause BM, Murphy CA, Uhlrich DJ, Banks MI (2017) PV+ Cells Enhance Temporal Population Codes but not Stimulus-Related Timing in Auditory Cortex. Cereb Cortex.

Langsjo JW, Alkire MT, Kaskinoro K, Hayama H, Maksimow A, Kaisti KK, Aalto S, Aantaa R, Jaaskelainen SK, Revonsuo A, Scheinin H (2012) Returning from oblivion: imaging the neural core of consciousness. J Neurosci 32:4935-4943.

Lee U, Ku S, Noh G, Baek S, Choi B, Mashour GA (2013) Disruption of frontal-parietal communication by ketamine, propofol, and sevoflurane. Anesthesiology 118:1264-1275.

Liu X, Lauer KK, Ward BD, Li SJ, Hudetz AG (2013) Differential effects of deep sedation with propofol on the specific and nonspecific thalamocortical systems: a functional magnetic resonance imaging study. Anesthesiology 118:59-69.

Liu X, Lauer KK, Ward BD, Rao SM, Li SJ, Hudetz AG (2012) Propofol disrupts functional interactions between sensory and high-order processing of auditory verbal memory. Hum Brain Mapp 33:2487-2498.

Maksimow A, Silfverhuth M, Langsjo J, Kaskinoro K, Georgiadis S, Jaaskelainen S, Scheinin H (2014) Directional connectivity between frontal and posterior brain regions is altered with increasing concentrations of propofol. PLoS One 9:e113616.

Manita S, Suzuki T, Homma C, Matsumoto T, Odagawa M, Yamada K, Ota K, Matsubara C, Inutsuka A, Sato M, Ohkura M, Yamanaka A, Yanagawa Y, Nakai J, Hayashi Y, Larkum ME, Murayama M (2015) A Top-Down Cortical Circuit for Accurate Sensory Perception. Neuron 86:1304-1316.

Mashour GA, Hudetz AG (2017) Bottom-Up and Top-Down Mechanisms of General Anesthetics Modulate Different Dimensions of Consciousness. Front Neural Circuits 11:44.

Meyer JF, Golshani P, Smirnakis SM (2018) The Effect of Single Pyramidal Neuron Firing Within Layer 2/3 and Layer 4 in Mouse V1. Front Neural Circuits 12:29.

Mitzdorf U (1985) Current source-density method and application in cat cerebral cortex: investigation of evoked potentials and EEG phenomena. Physiol Rev 65:37-100.

454 Murayama M, Pérez-Garci E, Nevian T, Bock T, Senn W, Larkum ME (2009) Dendritic
455 encoding of sensory stimuli controlled by deep cortical interneurons. Nature 457:1137-
456 1141.

457

458 Murphy C, Krause B, Banks M (2019) Selective effects of isoflurane on cortico-cortical
459 feedback afferent responses in murine non-primary neocortex. Br J Anaesth 123:488-
460 496.

461

462 Murphy CA, Krause BM, Grady SM, Banks MI (2017) Effect of isoflurane on selectively
463 activated afferent pathways in neocortex. In: Society for Neuroscience Annual Meeting.
464 Washington D.C., USA.

465

466 Nourski KV, Steinschneider M, Rhone AE, Kawasaki H, Howard MA, 3rd, Banks MI (2018)
467 Auditory Predictive Coding across Awareness States under Anesthesia: An Intracranial
468 Electrophysiology Study. J Neurosci 38:8441-8452.

469

470 Nourski KV, Banks MI, Steinschneider M, Rhone AE, Kawasaki H, Mueller RN, Todd MM,
471 Howard MA, 3rd (2017) Electrocorticographic delineation of human auditory cortical
472 fields based on effects of propofol anesthesia. Neuroimage 152:78-93.

473

474 Pettersen KH, Devor A, Ulbert I, Dale AM, Einevoll GT (2006) Current-source density
475 estimation based on inversion of electrostatic forward solution: effects of finite extent of
476 neuronal activity and conductivity discontinuities. JNeurosciMethods 154:116-133.

477

478 Picchioni D, Pixa ML, Fukunaga M, Carr WS, Horovitz SG, Braun AR, Duyn JH (2014)
479 Decreased connectivity between the thalamus and the neocortex during human
480 nonrapid eye movement sleep. Sleep 37:387-397.

481

482 Pouille F, Scanziani M (2001) Enforcement of temporal fidelity in pyramidal cells by somatic
483 feed- forward inhibition. Science 293:1159-1163.

484

485 Raz A, Grady SM, Krause BM, Uhlrich DJ, Manning KA, Banks MI (2014) Preferential effect of
486 isoflurane on top-down versus bottom-up pathways in sensory cortex. Front Syst
487 Neurosci 8.

488

489 Redinbaugh MJ, Phillips JM, Kambi NA, Mohanta S, Andryk S, Dooley G, Afrasiabi M, Raz A,
490 Saalmann Y (2020) Thalamus Modulates Consciousness Via Layer-Specific Control of
491 Cortex. Neuron 105.

492

493 Sanders RD, Banks MI, Darracq M, Moran R, Sleigh J, Gosseries O, Bonhomme V, Brichant
494 JF, Rosanova M, Raz A, Tononi G, Massimini M, Laureys S, Boly M (2018) Propofol-
495 induced unresponsiveness is associated with impaired feedforward connectivity in
496 cortical hierarchy. Br J Anaesth 121:1084-1096.

Sermet BS, Truschow P, Feyerabend M, Mayrhofer JM, Oram TB, Yizhar O, Staiger JF, Petersen CCH (2019) Pathway-, layer- and cell-type-specific thalamic input to mouse barrel cortex. eLife 8:e52665.

Suzuki M, Larkum ME (2020) General Anesthesia Decouples Cortical Pyramidal Neurons. Cell 180:666-676.e613.

Takahashi N, Oertner TG, Hegemann P, Larkum ME (2016) Active cortical dendrites modulate perception. Science 354:1587-1590.

Viaene AN, Petrof I, Sherman SM (2011a) Synaptic properties of thalamic input to layers 2/3 and 4 of primary somatosensory and auditory cortices. JNeurophysiol 105:279-292.

Viaene AN, Petrof I, Sherman SM (2011b) Properties of the thalamic projection from the posterior medial nucleus to primary and secondary somatosensory cortices in the mouse. Proc Natl Acad Sci USA 108:18156-18161.

Xie Z, McMillan K, Pike CM, Cahill AL, Herring BE, Wang Q, Fox AP (2013) Interaction of anesthetics with neurotransmitter release machinery proteins. Journal of neurophysiology 109:758-767.

Xu X, Olivas ND, Ikrar T, Peng T, Holmes TC, Nie Q, Shi Y (2016) Primary visual cortex shows laminar-specific and balanced circuit organization of excitatory and inhibitory synaptic connectivity. Journal of Physiology 594:1891-1910.

Xue M, Atallah BV, Scanziani M (2014) Equalizing excitation–inhibition ratios across visual cortical neurons. Nature 511:596.

Figure 1

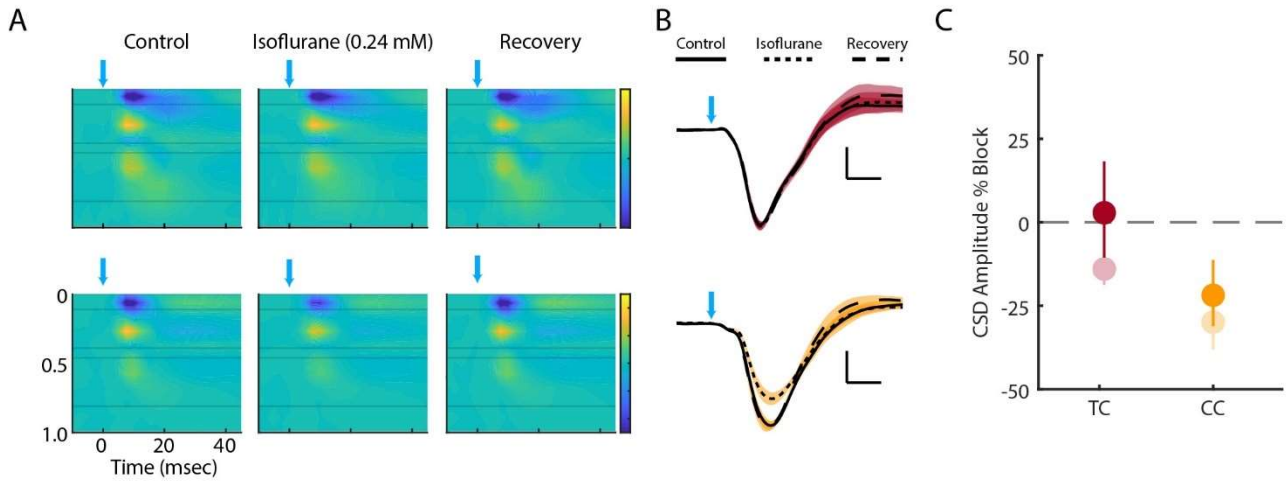

Figure 1. Effects of isoflurane on optogenetically evoked current sinks in layer 1 are pathway-specific. *A.* CSD color plots comparing evoked synaptic responses to a 2 msec light pulse (blue arrows) across control (*A*, left column), 0.24 mM isoflurane (*A*, middle column), and recovery (*A*, right column) for representative examples for TC (top row) and CC (bottom row) afferents; color scale: -5.0 to 5.0 μA mm^{-3}. *B.* Signals from layer 1 were used to compare synaptic effects across control (solid), 0.24 mM isoflurane (dotted), and recovery (dashed). Shaded regions indicate ± 1 SD among trials. *C.* Model fits of percent block of layer 1 sink by isoflurane with 95% confidence interval (vertical line). Responses evoked by stimulation of CC afferents to cortical layer 1 (orange) are suppressed to a greater extent under isoflurane than TC inputs (red). Pale markers reflect estimates of block by isoflurane at 0.24 mM based on results from Murphy et al., 2019. Raw values of CSD sink amplitudes under control conditions are shown in **Table 1.**

Figure 2

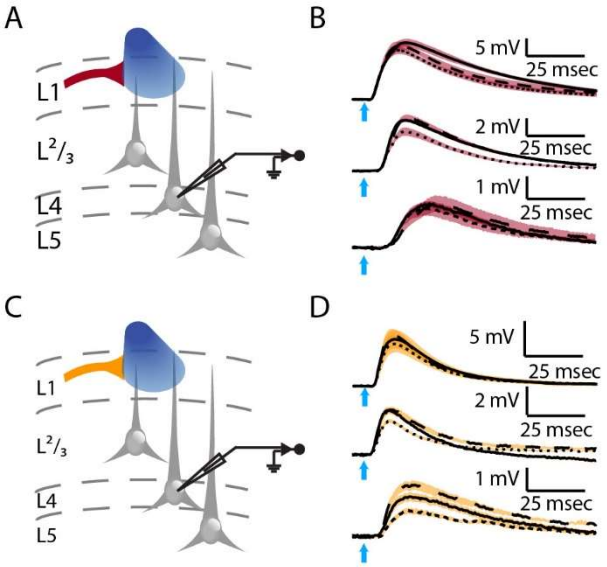

Figure 2. Example recordings from cortical pyramidal cells in response to activation of two distinct layer 1 afferents. *A.* Schematic demonstrating recordings conducted for panel *B*. TC afferents originating in the posterior medial nucleus of the thalamus were optogenetically activated while whole cell patch clamp recordings were conducted in pyramidal cells in L2/3, L4, or L5. *B.* Example recordings of TC-evoked responses from L2/3 (top), L4 (middle), or and L5 (bottom) cells during control (solid), 0.24 mM isoflurane (dotted), and recovery (dashed) conditions. Shaded regions indicate ± 1 SD among trials. *C-D*. Same as *A-B* for responses to CC inputs originating in cingulate cortex. Population results of isoflurane effects are shown in **Figure 3.** Raw values for control conditions are shown in **Table 2.**

Figure 3

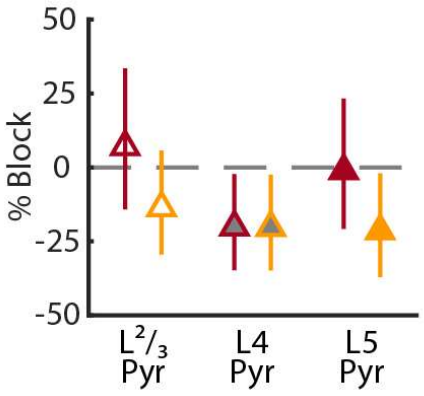

Figure 3. Suppression of post-synaptic responses by isoflurane is cell type-specific. Model estimates of the percent block by isoflurane of post-synaptic responses evoked by TC (red) or CC (orange) inputs to L2/3, L4, and L5 cell populations. Estimates are represented by triangles; vertical lines span 95% confidence intervals for isoflurane effects for each pathway-cell type combination, where confidence intervals overlapping 0% block are not significant (P>0.05). Both TC and CC inputs to L4 pyramidal cells were suppressed by isoflurane, as were CC inputs to L5 pyramidal cells. Effects are also quantified in **Table 3.**

Figure 4

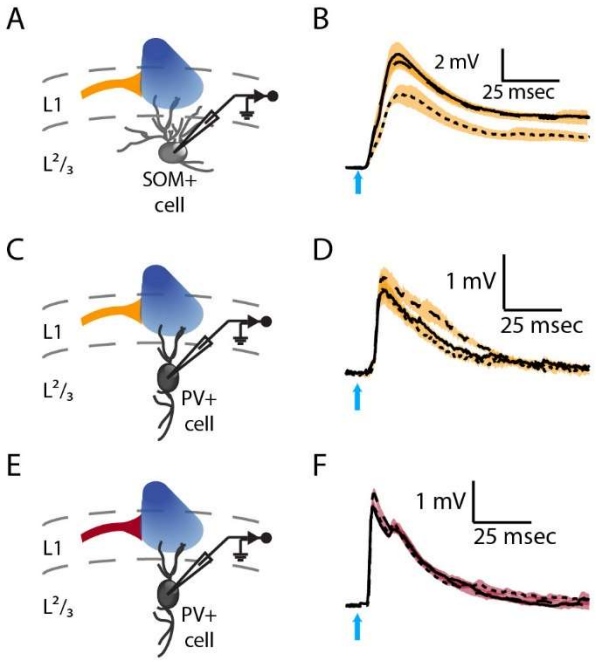

Figure 4. Example recordings from SOM+ and PV+ interneurons in response to activation of distinct layer 1 afferents. *A*. Schematic demonstrating recordings conducted for panel *B*. CC afferents to layer 1 were optogenetically activated while whole cell patch clamp recordings were conducted in SOM+ interneurons. *B*. Example recordings from CC-evoked responses in a SOM+ cell during control (solid), 0.24 mM isoflurane (dotted), and recovery (dashed) conditions. Shaded regions indicate ± 1 SD among trials. *C-D*. Same as *A-B* for CC inputs to PV+ cells. *E-F*. Same as A-B for TC inputs to PV+ cells. Note that examples of TC inputs to SOM+ cells are not shown, as TC inputs failed to evoke synaptic responses in SOM+ cells. Population results of isoflurane effects are shown in **Figure 5.** Raw values of PSP amplitude during control conditions are shown in **Table 2.**

Figure 5

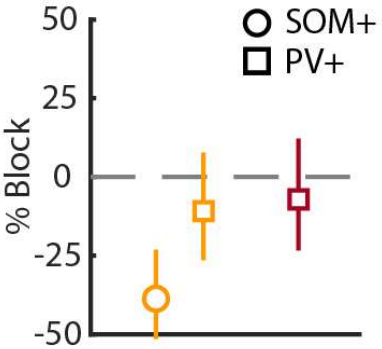

Figure 5. CC feedback inputs to SOM+ interneurons are suppressed by isoflurane, while TC and CC inputs to PV+ interneurons are not. Model estimates of the percent block by isoflurane of post-synaptic responses evoked by TC (red) or CC (orange) inputs to SOM+ and PV+ interneuron populations. Estimates are represented by circles (SOM+) or squares (PV+); vertical lines span 95% confidence intervals for isoflurane effects for each pathway-cell type combination, where confidence intervals overlapping 0% block are not significant (P>0.05). CC inputs to SOM+ cells were suppressed by isoflurane, but no effect of isoflurane was detected in TC nor CC inputs to PV+ cells. Effects are also quantified in **Table 3.**

Figure 6

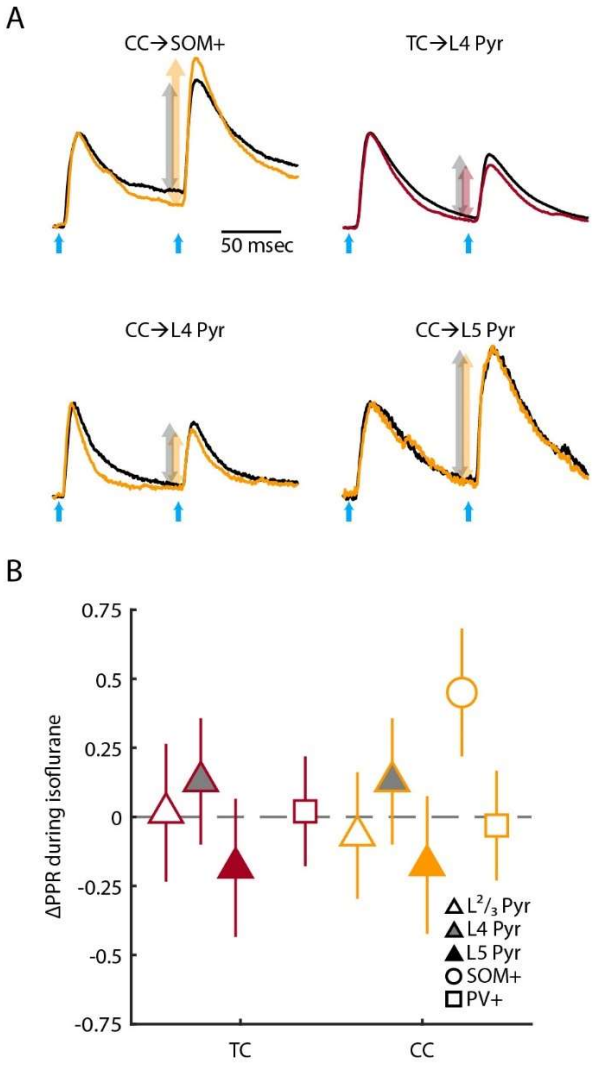

Figure 6. Isoflurane increases paired pulse ratios for CC inputs to SOM+ cells, suggest pre-synaptic mechanisms. *A.* Examples recordings from the four different pathway-cell type pairs that demonstrated suppression of synaptic responses by isoflurane. Responses for control (black) and isoflurane (either orange (CC) or red (TC)) conditions are normalized to the amplitude of the first pulse under control conditions to demonstrate paired pulse effects. Arrows show comparison of paired pulse effects between control (black) and isoflurane (either orange or red) conditions. *B.* Model estimates of the changes to paired pulse ratio during isoflurane, where positive values represent higher paired pulse ratios during isoflurane. Estimates of isoflurane effects on paired pulse ratios for responses evoked by TC (red) or CC (orange) inputs to all recorded populations are shown. Estimates are represented by shapes; vertical lines span 95% confidence intervals for isoflurane effects for each pathway-cell type combination, where confidence intervals overlapping 0 are not significant (P>0.05). Paired pulse ratios for CC inputs to SOM+ cells were enhanced by isoflurane, suggesting isoflurane blocks synaptic responses to SOM+ cells through pre-synaptic mechanisms. Raw values of PPR during control conditions are shown in **Table 2**, and isoflurane effects are quantified in **Table 5.**

Figure 7

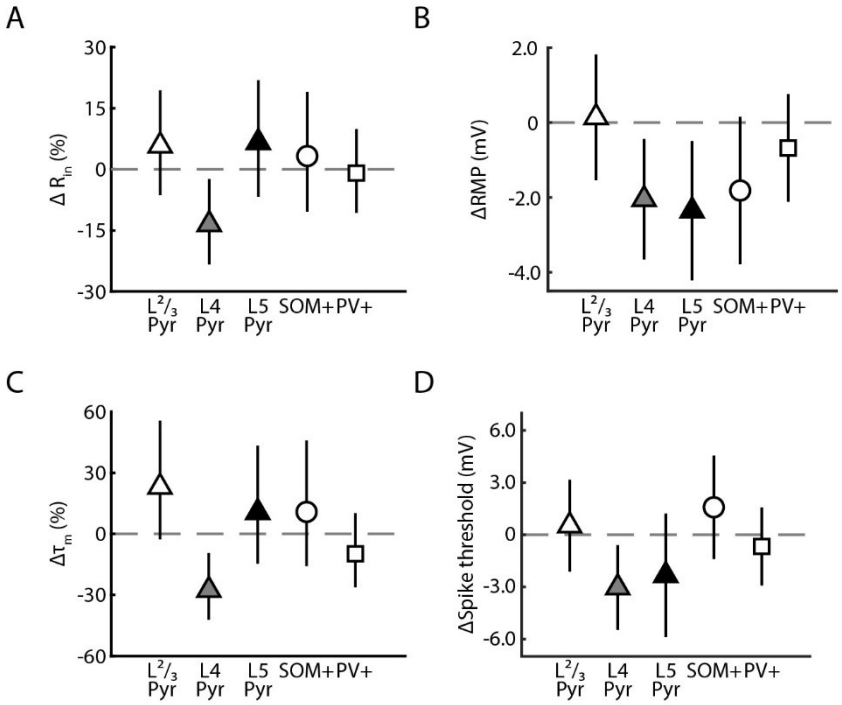

Figure 7. Isoflurane alters intrinsic membrane properties of L4 pyramidal cells, suggesting a shared mechanism by which TC and CC inputs are blocked. *A.* Model estimates of percent change of input resistance during isoflurane, where negative values represent decreases in input resistance (i.e., increased conductance). *B.* Model estimates of shifts of resting membrane potential during isoflurane, where negative values represent hyperpolarization of membrane potentials during isoflurane compared to baseline values. *C*. Same as in *A* for percent changes in membrane time constants. *D.* Same as in *B* for spike thresholds. L4 pyramidal cells became leakier (i.e., lower input resistances and shorter time constants) during isoflurane relative to baseline. Raw values of intrinsic properties during control conditions are shown in **Table 4.**

Table 1

	Latency (msec)	L1 sink amplitude ($\mu A \cdot mm^{-3}$)	% Block by isoflurane [95% CI]	P-value
TC	3.81±0.52	6.18±1.64	+2.9 [-10.6 18.3]	0.69
CC	3.61±0.56	5.33±1.35	-21.8 [-31.1 -11.3]	0.00026

Table 1. Activation of cortical afferents evokes short latency current sinks in layer 1 that are sensitive to isoflurane in a pathway-dependent manner. Layer 1 current sink amplitudes evoked by activation of CC inputs were suppressed by isoflurane, while those evoked by TC inputs were not. Estimates are based on predicted values from linear mixed effects model (see Methods).

Table 2

	PSP amplitude	PSP latency	PPR
TC→			
$L^2/_3$ Pyr (n=5)	2.4±1.8	5.9±2.3	0.86±0.33
L4 Pyr (n=6)	4.1±2.3	5.6±1.6	0.64±0.23
L5 Pyr (n=5)	8.3±5.7	5.4±1.8	0.77±0.29
SOM+ (n=2)	5.1±4.5	3.0±0.5	0.61±0.04
PV+ (n=8)	6.4±2.3	4.1±0.7	0.68±0.25
CC→			
$L^2/_3$ Pyr (n=6)	2.0±1.4	4.6±1.2	0.57±0.30
L4 Pyr (n=6)	4.6±4.6	4.8±1.2	0.79±0.27
L5 Pyr (n=5)	2.6±1.7	6.5±1.8	1.05±0.34
SOM+ (n=6)	6.5±5.0	4.6±0.7	0.74±0.45
PV+ (n=8)	4.3±4.8	4.9±1.2	0.78±0.32

Table 2. Properties of evoked responses in whole cell patch clamp recordings conducted during control conditions in pyramidal cells and interneurons. Values shown are mean ± standard deviation. Latency was calculated relative to onset of 2 msec light pulse. Paired pulse ratios were calculated as the amplitude of the 2nd post-synaptic potential (relative to the pre-response baseline) divided by the baseline subtracted amplitude of the 1st post-synaptic potential.

Table 3

	% Block	95% CI	P-value
TC→			
$L^2/_3$ Pyr	7.0	[-14.2 33.5]	0.54
L4 Pyr	-20.1	[-34.7 -2.3]	0.029
L5 Pyr	-1.1	[-20.7 23.3]	0.92
PV+	-6.6	[-21.6 11.3]	0.44
CC→			
$L^2/_3$ Pyr	-13.6	[29.4 5.7]	0.15
L4 Pyr	-20.3	[-34.8 -2.4]	0.028
L5 Pyr	-21.5	[-37.0 -2.0]	0.033
SOM+	-35.8	[-47.5 -21.4]	<0.0001
PV+	-10.0	[-24.5 7.2]	0.23

Table 3. Isoflurane affects synaptic responses in a cell type-dependent manner. Estimates are based on predicted values from linear mixed effects model (see Methods). Values represent the percent change in the amplitude of post-synaptic responses during isoflurane relative to baseline conditions. Negative values represent suppression of synaptic responses by isoflurane.

Table 4

	RMP (mV)	R_{in} (MΩ)	τ_m (msec)	Spike Threshold (mV)
$L^2/_3$ Pyr (n=11)	-71.5±3.6	114.2±45.9	14.1±10.7	-43.1±4.0
L4 Pyr (n=12)	-68.9±5.3	183.2±103.8	19.0±13.2	-41.9±6.1
L5 Pyr (n=10)	-65.1±3.7	135.77±85.9	18.0±9.8	-41.8±5.3
SOM+ (n=8)	-60.3±6.2	317.3±138.8	38.2±38.0	-42.2±3.9
PV+ (n=16)	-63.5±4.0	166.8±47.1	9.6±2.5	-46.3±7.9

Table 4. Intrinsic properties of recorded cell types during control conditions. Values are mean ± standard deviation. Properties were measured ~2 minutes after achieving whole cell access. A series of 10-20 current steps (600 msec) was delivered at progressive intervals (10-40 pA), beginning with a hyperpolarizing current injection. Resting membrane potentials (RMP) were calculated by averaging membrane potentials in the 100 msec prior to onset of all current pulses. Input resistances (R_{in}) were extrapolated from relationship between current and steady state voltages. Time constants (τ_m) were estimated using the first hyperpolarizing current pulse. Spike thresholds were evaluated using the first trial to evoke an action potential, where the spike threshold was the voltage at which the second derivative exceeded twice the standard deviation of the pre-spike baseline value.

Table 5

	ΔPPR	95% CI	P-value
TC→			
$L^2/_3$ Pyr	+0.02	[-0.32 0.26]	0.90
L4 Pyr	+0.13	[-0.10 0.36]	0.27
L5 Pyr	-0.18	[-0.43 0.07]	0.15
PV+	+0.02	[-0.18 0.22]	0.84
CC→			
$L^2/_3$ Pyr	-0.07	[-0.30 0.16]	0.56
L4 Pyr	+0.13	[-0.10 0.36]	0.27
L5 Pyr	-0.18	[-0.42 0.08]	0.17
SOM+	+0.45	[0.22 0.68]	0.0002
PV+	-0.03	[-0.23 0.17]	0.76

Table 5. Isoflurane alters short-term synaptic plasticity for CC inputs to SOM+ interneurons. Estimates are based on predicted values from linear mixed effects model (see Methods) and represent the change in PPR (in mV) relative to baseline PPR. Negative values represent decreases in PPR (e.g., stronger paired pulse depression) during isoflurane.